Hydrocarbon-Enriched Bio-oil from Catalytic Microwave Pyrolysis of Macaúba Epicarp

Reginaldo J. Cavallaro
Instituto Federal do Sudeste de Minas Gerais
Carla E. Hori
Federal University of Uberlândia
Claudio R. Duarte
Federal University of Uberlândia
Marcos A. S. Barrozo
masbarrozo@ufu.br

Federal University of Uberlândia

Research Article

Keywords: macauba, catalytic pyrolysis, microwave-assisted pyrolysis, bio-oil, biochar

Posted Date: March 9th, 2026

DOI: https://doi.org/10.21203/rs.3.rs-8105883/v1

Additional Declarations: No competing interests reported.

Version of Record: A version of this preprint was published at Biomass Conversion and Biorefinery on July 7th, 2026. See the published version at https://doi.org/10.1007/s13399-026-07194-8.

Abstract

Microwave-assisted pyrolysis (MAP) of Acrocomia aculeata epicarp (EPM) was investigated using an ex situ catalytic configuration supported on silicon carbide (SiC) foams. The study employed acidic, basic, and bifunctional catalysts, including CaO, phosphate rock residue (PO), Nb_2O_5, NiO/Nb_2O_5, and zeolite. The primary objective was to elucidate the catalytic effects on product selectivity, the reduction of oxygenated compounds, and the promotion of hydrocarbons in the resulting bio-oils. Optimization of the non-catalytic pyrolysis indicated that 550°C was the ideal temperature, yielding 48.4% condensables, 20.6% biochar, and 32.3% gases. Among the catalysts tested, the bifunctional NiNb–PO system achieved the highest hydrocarbon fraction (61.3%) and the lowest oxygenated content (35.4%), demonstrating a synergistic interaction between basic and redox sites. Basic catalysts such as CaO and PO enhanced decarboxylation and decarbonylation reactions, while Nb_2O_5 and NiNb-based systems favored selective hydrogenation and deoxygenation. In contrast, zeolite-containing systems exhibited higher acidity and a propensity to form oxygenated intermediates. The resulting biochar presented a high fixed carbon content (up to 42.5%), a low O/C ratio (0.24), and a higher heating value (21.55 MJ kg^{-1}), indicating the formation of an aromatic, porous, and stable carbon matrix suitable for energy and environmental applications. This work demonstrates that integrating multifunctional catalysts, conductive SiC supports, and microwave heating provides a technically viable and environmentally sustainable route for producing hydrocarbon-enriched bio-oils and high-performance biochars from tropical lignocellulosic residues, supporting the advancement of low-carbon bioenergy technologie.

1. Introduction

The increasing global reliance on fossil fuels has created significant environmental, economic, and strategic challenges. The intensive extraction of petroleum, coal, and natural gas constitutes an unsustainable model that drives greenhouse gas emissions, ecosystem degradation, and climate instability [1]. Consequently, these issues have accelerated the search for alternative and sustainable energy systems capable of supporting economic development while meeting international decarbonization targets [2].

Lignocellulosic biomass has emerged as a strategic renewable resource owing to its abundance, versatility, and potential for carbon neutrality when managed sustainably. Agricultural and agro-industrial residues already contribute approximately 14% of the global energy supply and are increasingly utilized in thermochemical conversion processes to produce fuels and high-value chemicals [3, 4]. In Brazil, where renewable sources comprise 47.4% of the national energy matrix—a figure substantially higher than the global average [5]—the vast availability of agricultural and forestry residues reinforces the nation's comparative advantage for expanding bioenergy production during the ongoing energy transition.

Among various thermochemical routes, pyrolysis stands out as a highly promising technology due to its capacity to simultaneously generate bio-oil, biochar, and syngas. These products offer diverse

applications, from alternative liquid fuels to chemical precursors and soil conditioners [6]. Nevertheless, the widespread adoption of bio-oil is hindered by several unfavorable properties, including high oxygen content, low energy density, elevated acidity, and poor storage stability [7].

To address these limitations, catalytic pyrolysis has emerged as an effective upgrading strategy. Appropriate catalysts can facilitate deoxygenation, cracking, and selective aromatization reactions, thereby improving bio-oil quality to yield liquid fuels with energy densities and stability comparable to those of conventional fossil fuels [8, 9]. A wide range of materials—including zeolites, metal oxides, and bifunctional systems—have been investigated for this purpose, each demonstrating distinct performance characteristics regarding selectivity, stability, and cost [10, 11].

The valorization of non-conventional biomass from tropical biomes like the Brazilian Cerrado remains a largely underexplored frontier. Recognized as a global biodiversity hotspot, the Cerrado hosts a rich diversity of plant species and generates significant quantities of agro-industrial residues that are often underutilized [12]. This biome contains approximately 4,400 plant species, yet only about 30% have been characterized for potential applications.

Acrocomia aculeata (macauba), a palm native to this region, produces fruit with components of notable economic value. While its kernel is a source of oil and protein-rich meal, the residual biomass—particularly the epicarp and endocarp—constitutes a valuable by-product with yields reaching up to 10 t ha^{-1} yr^{-1}. The epicarp, which is the focus of this work, possesses high energy potential [13]. Consequently, macauba has been identified as a promising feedstock for biofuel production. For instance, Cavallaro et al. [14] reported that the catalytic micropyrolysis of macauba epicarp and endocarp using catalysts such as CaO, Nb_2O_5, and Ni/Nb_2O_5 leads to significant hydrocarbon formation. These catalysts enhance deoxygenation and increase the fraction of aliphatic and aromatic hydrocarbons in the resulting bio-oil. Therefore, the valorization of macauba biomass contributes to advanced residue management and supports the development of sustainable biofuel technologies.

In this context, microwave-assisted pyrolysis (MAP) has emerged as an innovative alternative to conventional heating. MAP offers efficient volumetric heating, improved thermal uniformity, and suppression of undesired secondary reactions, thereby enhancing energy efficiency and reducing process residence time [15]. These advantages make it an attractive route for lignocellulosic residue valorization at both laboratory and industrial scales.

Accordingly, this study investigates the ex situ catalytic pyrolysis of macauba epicarp biomass (EPM) via microwave heating, with catalysts supported on silicon carbide (SiC) foam. A range of acidic, basic, and bifunctional catalysts—including calcium oxide (CaO), phosphate rock residue (PO), niobium oxide (Nb_2O_5), nickel oxide on Nb_2O_5 (NiO/Nb_2O_5), and zeolite—were evaluated. The primary objective was to elucidate the interactions between these catalysts and pyrolysis intermediates while assessing their influence on product selectivity, oxygenate reduction, and the formation of hydrocarbons. Furthermore, the physicochemical properties of the resulting bio-oil and biochar were analyzed to determine their suitability for energy applications.

By integrating an alternative biomass with innovative catalysts and microwave-assisted pyrolysis, this work contributes to a deeper understanding of the mechanisms governing the valorization of tropical lignocellulosic residues. The findings offer technological insights that support scientific advancement, enable more efficient catalytic cracking pathways, and reinforce the transition toward a low-carbon energy economy.

2. Material and Methods

2.1. Feedstock preparation and characterization

The epicarp of macauba (EPM), sourced from the Cerrado biome in Araxá, Minas Gerais, Brazil, was used as the lignocellulosic feedstock. The raw material was manually cleaned to remove impurities, washed with deionized water, and dried in a forced-air oven at 80°C for 48 h. The dried biomass was then milled and sieved to a particle size range of 0.21–0.25 mm. All characterization analyses were performed in triplicate to ensure reproducibility.

The macauba fruit exhibits a spherical morphology composed of four distinct parts: epicarp, mesocarp, endocarp, and endosperm [16, 17]. The morphological structure of the fruit is presented in Fig. 1.

Proximate Analyses: Moisture, volatile matter, fixed carbon, and ash contents were determined following ASTM standards E871-82, E872-82, and D1102-84. Elemental composition (C, H, N, S) was measured using a PerkinElmer 2400 Series II CHNS analyzer, with oxygen content calculated by difference. The higher heating value (HHV) was determined using an IKA C2000 adiabatic bomb calorimeter.

Thermogravimetric analysis (TGA) and differential scanning calorimetry (DSC) were performed on a Netzsch STA 449 F3 instrument to assess thermal stability. Samples were heated to 900°C at a rate of 10°C min^{-1} under a nitrogen flow of 20 mL min^{-1}. Surface functional groups were identified using a Bruker Tensor 27 FTIR-ATR spectrometer (4000–400 cm^{-1}). Inorganic composition and surface morphology were examined via X-ray fluorescence (XRF) spectroscopy (Shimadzu EDX-720) and scanning electron microscopy (SEM) (JEOL JSM-6510LV), respectively.

2.2. Catalysts and support preparation

This study employed an ex situ catalytic configuration, where pyrolysis vapors were directed to a secondary catalytic bed. This setup was chosen to minimize catalyst deactivation and facilitate recovery [18]. The catalysts investigated included calcium oxide (CaO), phosphate rock residue (PO), niobium pentoxide (Nb_2O_5), nickel oxide on Nb_2O_5 (NiO/Nb_2O_5), and a commercial zeolite. These were selected to evaluate the effects of basic (CaO), acidic (Nb_2O_5, zeolite), and bifunctional (NiO/Nb_2O_5) properties on bio-oil composition.

The principal catalytic reactions during pyrolysis include deoxygenation (decarboxylation, decarbonylation, and dehydration), aromatization, and catalytic cracking. Deoxygenation is particularly

relevant for improving bio-oil quality by reducing oxygenated compound content through the following pathways:

- Decarboxylation: Removal of carboxyl groups producing CO_2 (R-COOH → CO_2 + RH) [19].
- Decarbonylation: Elimination of carbonyl groups with CO formation (R-CHO → CO + RH) [20].
- Dehydration: Elimination of water molecules leading to unsaturated or aromatic compounds (R-CH_2-CH_2OH → R-CH = CH_2 + H_2O).
- Aromatization: Conversion of aliphatic hydrocarbons into aromatic structures.
- Catalytic cracking: Fragmentation of long-chain hydrocarbons into lighter molecules (R_1–R_2 → R_1–H + R_2–H) [19].

Catalyst Support: Open-cell silicon carbide (SiC) foam disks were used as the catalyst support material due to their high thermal conductivity, mechanical strength, and chemical inertness [21, 22]. This structure ensures efficient heat distribution and adequate permeability for vapor-phase transport.

Catalyst Deposition: Two configurations were prepared: single-catalyst and dual-catalyst beds. For single-bed systems, 3.0 ± 0.15 g of a single catalyst was deposited onto a pre-dried SiC foam disk via wet impregnation using 70% ethanol as a binding agent. For dual-bed systems, a total of 3.0 ± 0.15 g of catalyst was used, with each side of the SiC foam disk impregnated with 1.5 g of a different catalyst, as detailed in Table 1.

Table 1
Identification of dual-catalyst bed experiments.

Experiment	Catalyst 1	Catalyst 2
Zeo–CaO	Zeolite	CaO
Zeo–PO	Zeolite	Phosphate residue
Zeo–Nb	Zeolite	Nb_2O_5
Zeo–NiNb	Zeolite	NiO/Nb_2O_5
CaO–PO	CaO	Phosphate residue
CaO–Nb	CaO	Nb_2O_5
CaO–NiNb	CaO	NiO/Nb_2O_5
Nb–PO	Nb_2O_5	Phosphate residue
Nb–NiNb	Nb_2O_5	NiO/Nb_2O_5
NiNb–PO	NiO/Nb_2O_5	Phosphate residue

2.3. Microwave pyrolysis system and procedure

Pyrolysis experiments were conducted in a laboratory-scale microwave unit comprising a 1000 W, 2.45 GHz microwave generator (Menumaster MCS10TSB) coupled to a 750 mL quartz reactor (Fig. 2). Temperature was monitored using a K-type thermocouple inserted into the biomass bed and regulated by a PID controller. Before each run, the system was purged with N_2 (50 mL min^{-1} for 20 min) to ensure an inert atmosphere. A 60 ± 0.5 g sample of EPM was used for each experiment. Evolved vapors were directed through a condenser train to collect the bio-oil, while non-condensable gases were removed by a vacuum pump.

To determine the optimal process temperature, non-catalytic pyrolysis experiments were conducted at five temperatures (479, 500, 550, 600, and 621°C), with each run held for 30 min [23]. The optimal temperature identified from this analysis was subsequently adopted for all catalytic runs.

2.4. Product characterization

2.4.1. Bio-oil analysis

The collected condensable fraction was separated into aqueous and organic phases via decantation and centrifugation (5000 rpm). The organic phase was extracted with dichloromethane (1:35 bio-oil:solvent mass ratio) and analyzed using a Shimadzu GC/MS-QP2020 NX system equipped with an RTX-1701 capillary column (60 m × 0.25 mm × 0.25 μm). Helium (99.999%) was the carrier gas at a flow rate of 404 mL min^{-1} and a pressure of 115 kPa. The GC–MS interface and transfer line were maintained at 250°C and 280°C, respectively. Approximately 1.0 μL of the sample was injected. Compounds were identified using the NIST11 spectral library, with a similarity index threshold of > 80% [23, 24]. Detected compounds were classified as oxygenates, nitrogenates, or hydrocarbons.

2.4.2. Biochar characterization

The elemental composition (C, H, O) of the biochar was estimated using the correlations developed by Nhuchhen [25]. Structural properties were investigated using a Shimadzu IR Prestige-21 FTIR spectrophotometer (4000–400 cm^{-1}, KBr pellets). The degree of aromaticity and carbonization was further assessed by constructing a Van Krevelen diagram.

2.4.3. Higher Heating Value (HHV) determination

The HHV of the feedstock, biochar, and condensable products was determined in triplicate using an IKA C2000 adiabatic bomb calorimeter following the ASTM D2015 standard.

3. Results and Discussion

3.1. Feedstock characterization

The physicochemical characterization of the macauba epicarp (EPM), summarized in Table 2, confirms its suitability for thermochemical conversion. Specifically, its high volatile matter (79.65%) and low ash

(1.35%) contents indicate a strong potential for high bio-oil yield. Furthermore, these properties are consistent with values previously reported in the literature for this biomass [16, 26].

Table 2
Characteristics of the Macaúba Epicarp (EPM)

	This Work	Evaristo et al. [16]	Dourado et al. [26]
Moisture (%) (db)	6.50 (± 0.02)	--	--
Ash (%)	1.35 (± 0.04)	3.69	--
Volatile matter (%)	79.65 (± 0.17)	81.60	--
Fixed carbon (%)	18.99 (± 0.16)	14.70	--
Carbon (%)	48.34 (± 3.21)	47.20	47.16
Hydrogen (%)	5.93 (± 3.79)	7.26	5.89
Oxygen (%)	43.69 (± 3.74)	42.05	46.95
HHV ($MJ \bullet kg^{-1}$)	18.32 (± 0.71)	20.24	19.27

The thermal decomposition profile of EPM was evaluated by TGA and DTG analysis (Fig. 4). The DTG curve reveals three main decomposition stages: moisture removal (< 150°C), degradation of hemicellulose and cellulose (220–400°C), and slow decomposition of remain lignin (> 400°C) [27]. The most significant mass loss (~ 60%) occurred between 150°C and 380°C, with a maximum degradation rate observed at approximately 350°C, corresponding to the decomposition of holocellulose. Above 400°C, the mass loss rate slowed considerably, characteristic of lignin's recalcitrant structure, leaving a final char residue of approximately 23% at 800°C [28, 29]. This multistage decomposition behavior is typical of lignocellulosic biomass and provides valuable information for understanding its thermal conversion.

3.2. Catalyst characterization

The elemental composition of the catalysts, determined by XRF, is presented in Table 3. The results confirm the distinct chemical nature of each material, which governs its catalytic function. The CaO-based catalyst with CaO as its main component (79.60%), providing strong basic sites for deoxygenation [30]. In contrast, the phosphate rock (PO) presented a complex mixture of CaO (22.43%), Fe_2O_3 (29.38%), and P_2O_5 (17.31%), indicating multifunctional properties suitable for promoting redox and acid-base reactions [31]. The high purity of Nb_2O_5 (99.24%) offers moderate Lewis acidity, while the NiO/Nb_2O_5 catalyst (3.98% NiO) combines this acidity with nickel's hydrogenation capabilities, creating a synergistic system for oxygen removal [32, 33]. The commercial zeolite exhibited a typical aluminosilicate composition (43.00% SiO_2, 24.26% Al_2O_3), providing strong acidic sites for cracking and aromatization.

Table 3
XRF Analysis – Catalyst Composition

Formula	Z	CaO	Phosphate rock residue	Nb_2O_5	$NiONb_2O_5$	Zeolite
Na_2O	11	--	--	--	--	14.96%
MgO	12	1.11%	0.95%	--	--	2.04%
Al_2O_3	13	0.16%	1.79%	--	--	24.26%
SiO_2	14	0.55%	10.82%	--	--	43.00%
P_2O_5	15	0.13%	17.31%	--	--	0.17%
SO_3	16	--	1.06%	--	--	--
K_2O	19	--	--	--	--	0.16%
CaO	20	79.60%	22.43%	0.06%	0.05%	0.74%
TiO_2	22	--	8.13%	--	--	0.10%
Cr_2O_3	24	--	0.08%	--	--	--
MnO	25	--	0.59%	--	--	--
Fe_2O_3	26	0.09%	29.38%	0.06%	0.07%	0.70%
NiO	28	--	0.04%	--	3.98%	--
CuO	29	0.02%	0.04%	0.05%	0.04%	0.02%
ZnO	30	0.01%	0.07%	0.01%	--	--
Br	35	0.60%	0.17%	0.28%	0.18%	--
SrO	38	0.22%	0.61%	--	--	--
$Y2O_3$	39	--	0.03%	0.04%	0.04%	--
ZrO_2	40	--	0.38%	--	0.70%	--
Nb_2O_5	41	--	0.42%	99.24%	94.57%	--
MoO_3	42	--	--	0.26%	0.21%	--
BaO	56	--	4.19%	--	--	--
La_2O_3	57	--	0.37%	--	0.16%	0.15%
Pr_6O_{11}	59	--	3 PPM	--	--	--

Formula	Z	CaO	Phosphate rock residue	Nb_2O_5	$NiONb_2O_5$	Zeolite
ThO_2	90	--	0.05%	--	--	--

Overall, the XRF results confirm that the elemental composition plays a determining role in modulating catalytic properties: CaO and PO provide basic and mixed functions, while Nb_2O_5 and NiO/Nb_2O_5 offer balanced redox and acidic characteristics, and zeolite provides strong acidity.

3.3. Non-catalytic pyrolysis

3.3.1 Effect of temperature on product distribution

The effect of temperature on product distribution during non-catalytic pyrolysis was investigated (Fig. 3). As the temperature increased from 479°C to 621°C, the biochar yield decreased from 32.3% to 20.6%, while the gas yield increased from 20.5% to 32.3%. This trend is attributed to the intensification of primary devolatilization and secondary cracking reactions at higher temperatures [34]. The bio-oil yield remained relatively stable, peaking at 48.4% at 550°C. Therefore, 550°C was selected as the best temperature for the subsequent catalytic experiments, as it maximized bio-oil yield.

3.3.2 Biochar characterization

The chemical transformations from biomass to biochar as a function of temperature were investigated by FTIR analysis (Fig. 4). The raw EPM spectrum shows characteristic lignocellulosic features, including a prominent O–H band (~ 3400 cm^{-1}), aliphatic C–H peaks (~ 2920 cm^{-1}), and a complex fingerprint region (1500–1000 cm^{-1}) rich in C–O stretching vibrations from cellulose and hemicellulose. Upon pyrolysis, a drastic structural change occurs. Even at 479°C, the O–H and aliphatic C–H bands are almost entirely eliminated, confirming extensive dehydration and devolatilization. Crucially, the effect of increasing temperature is most evident in the progressive simplification of the biochar spectra. As the temperature rises from 479°C to 621°C, the fingerprint region becomes progressively flatter, signifying the systematic removal of residual oxygen-containing functionalities (e.g., C–O, C–O–C) from the char matrix. While these oxygenated and aliphatic groups are removed, the band at ~ 1600 cm^{-1} (aromatic C = C stretching) is preserved and becomes the dominant feature in the spectra of biochars produced at higher temperatures (≥ 550°C). This trend reflects the progressive thermal evolution of the solid residue. An increase in pyrolysis temperature within the studied range results in a more advanced degree of carbonization, yielding a final product with a more ordered, highly aromatic, and stable carbon structure [25, 35]

3.3.3 Biochar composition and energy potential

The transformation of biomass into an energy-dense solid fuel is confirmed by the changes in its elemental composition and properties (Table 4). As pyrolysis temperature increased, the fixed carbon content rose significantly (from 18.9% to 42.5% at 621°C), which is directly explained by the evolution of

the atomic ratios. The O/C ratio decreased sharply from 0.65 in the biomass to an average of 0.26 in the biochars, indicating extensive deoxygenation through the removal of volatile compounds like H_2O, CO, and CO_2. This loss of oxygen is the primary driver for the increase in the higher heating value (HHV) from 18.32 to 21.55 MJ kg^{-1}. Simultaneously, the H/C ratio dropped from 1.45 to ~ 0.7, signifying a profound structural transformation towards aromatization. This change reflects the cleavage of aliphatic side chains and the formation of a more condensed, aromatic carbon matrix. Together, the reduction in both ratios, often visualized in a Van Krevelen diagram [34], demonstrates a clear pathway of carbonization, where the biomass evolves into a more stable, hydrophobic, and coal-like material.

Table 4
Composition of the biochar and atomic ratios

	EPM *in natura*	**479°C**	**500°C**	**550°C**	**600°C**	**621°C**
H/C	1.45	0.78	0.70	0.75	0.78	0.68
O/C	0.65	0.29	0.25	0.27	0.29	0.24
PCS (MJ/kg)	18.32	20.34	20.91	20.89	20.57	21.55
Ash (%)	1.3	12.7	13.5	11.5	11.8	11.9
Volatile matte (%)	79.6	50.0	45.8	49.4	50.5	45.6
Fixed carbon (%)	18.9	37.3	40.7	39.1	37.8	42.5

The significant increase in ash content, from 1.3% in the raw biomass to an average of 12.3% in the biochars (Table 4), is a direct consequence of the concentration of inorganic constituents as organic matter is volatilized. The XRF analysis (Table 5) provides a deeper insight into this process, revealing distinct behaviors among the elements. Thermally stable, refractory elements like Si and Al were concentrated in the biochar, as their oxides are not volatile at these temperatures. Conversely, elements known to form volatile species, such as K, S, and Cl, showed a relative decrease, indicating their partial loss to the gas phase during pyrolysis. This selective volatilization is beneficial, as it reduces elements linked to corrosion and harmful emissions (S, Cl) while concentrating others [36, 37].

Table 5
Effect of pyrolysis temperature on the elemental composition of biochar.

Element	EPM *in natura*	479°C	500°C	550°C	600°C	621°C
K	2.61%	2.18%	1.73%	2.24%	2.10%	2.10%
Si	0.32%	0.46%	0.38%	0.50%	0.68%	0.57%
Ca	0.92%	0.38%	0.31%	0.46%	0.45%	0.41%
Mg	0.16%	0.36%	0.25%	0.36%	0.40%	0.35%
Al	0.14%	0.30%	0.24%	0.32%	0.42%	0.36%
P	0.21%	0.28%	0.21%	0.29%	0.30%	0.27%
Fe	0.68%	0.14%	0.11%	0.15%	0.21%	0.18%
S	0.24%	0.06%	0.05%	0.05%	0.05%	0.05%
Cl	0.09%	0.06%	0.04%	0.06%	0.05%	0.05%
Ti	0.05%	0.02%	0.01%	0.02%	0.03%	0.02%
Rb	0.03%	38 PPM	28 PPM	41 PPM	38 PPM	39 PPM
Zn	0.03%	38 PPM	30 PPM	35 PPM	33 PPM	33 PPM
Cu	0.03%	37 PPM	27 PPM	34 PPM	35 PPM	31 PPM
Sr	0.04%	28 PPM	22 PPM	31 PPM	32 PPM	26 PPM
Mn	0.01%	25 PPM	19 PPM	--	24 PPM	23 PPM
Cr	--	20 PPM	20 PPM	21 PPM	21 PPM	18 PPM
Mo	0.07%	10 PPM	--	12 PPM	--	--
Zr	--	7 PPM	--	7 PPM	12 PPM	10 PPM
V	--	--	13 PPM	--	--	--
Ru	0.06%	--	24 PPM	--	--	--
Ni	--	--	--	9 PPM	--	--
Nb	--	--	--	--	5 PPM	17 PPM

3.3.4 Morphological analysis (SEM)

Scanning electron microscopy (SEM) revealed significant morphological changes following pyrolysis (Fig. 5). While the raw EPM surface appeared relatively smooth and fibrous, the biochar produced at 550°C exhibited a highly porous and heterogeneous structure. The formation of well-developed pores

and cavities is a direct result of the release of volatile matter during thermal decomposition. This porous matrix enhances the biochar's surface area, making it suitable for applications such as an adsorbent or catalyst support. The observed high density of interconnected pores and larger voids is associated with volatile removal and carbon matrix reorganization, which strongly influence the textural and reactive properties of the biochar.

3.4. Catalytic pyrolysis: single-bed configuration

The performance of individual catalysts in the ex situ upgrading of pyrolysis vapors was evaluated to establish a baseline for their intrinsic activity (Fig. 5). In the non-catalytic control run (550), the bio-oil was composed predominantly of oxygenated compounds (93.2%), with a negligible hydrocarbon fraction of only 5.4%. This confirms that, without catalytic intervention, the thermal decomposition of macauba epicarp primarily yields a complex mixture of acids, aldehydes, ketones, and phenols, which are characteristic of lignocellulosic pyrolysis.

All catalysts demonstrated deoxygenation activity, significantly increasing the hydrocarbon content. The basic catalysts, CaO and PO, were the most effective in the single-bed setup, yielding hydrocarbon fractions of 14.2% and 13.5%, respectively. This performance is attributed to their ability to promote decarboxylation and decarbonylation reactions, which are key pathways for C–O bond cleavage in carboxylic acids and carbonyls, effectively removing oxygen as CO_2 and CO [38]. This suggests that the initial pyrolysis vapors are rich in acidic compounds, which are readily neutralized and converted by these basic sites [39].

The NiO/Nb_2O_5 system showed intermediate performance (10.1% hydrocarbons). This indicates that its synergistic acidic and redox sites facilitated hydrogenation and subsequent hydrodeoxygenation (HDO). However, the limited hydrogen availability in a standard pyrolysis environment (without an external H_2 source) likely constrained its full potential. The lower performance of Nb_2O_5 and zeolite individually suggests that their acidic sites alone, while promoting cracking, were insufficient to drive deep deoxygenation, possibly leading to the formation of smaller, but still oxygenated, molecules.

Despite these improvements, oxygenated compounds remained the dominant fraction (> 85%) in all single-bed experiments. This highlights a fundamental limitation: a single catalytic function (e.g., basicity or acidity alone) is insufficient to address the chemical complexity of pyrolysis vapors. This observation motivated the investigation of dual-catalyst beds to combine complementary functions

3.5. Catalytic pyrolysis: dual-bed configuration

Dual-catalyst bed configurations were investigated to explore synergistic effects on bio-oil upgrading, aiming to create a multi-step reaction environment within a single pass (Fig. 6). All combinations significantly outperformed the single-bed systems, confirming the hypothesis that combining catalysts with complementary functions is a superior strategy.

The hydrocarbon fraction in the dual-bed systems varied from 15.5% to an impressive 61.3%, a more than tenfold increase compared to the non-catalytic control (5.4%). The NiNb–PO system was exceptionally effective, achieving the highest hydrocarbon fraction (61.3%) and drastically reducing the oxygenate content to 35.4%. This remarkable result is attributed to a powerful synergistic cascade:

a. The pyrolysis vapors first encounter the phosphate rock (PO), whose basic and multifunctional sites neutralize acidic compounds and promote initial decarboxylation/decarbonylation.
b. The partially deoxygenated intermediates then flow to the NiO/Nb_2O_5 catalyst, where the redox/acidic sites facilitate hydrogenation and final hydrodeoxygenation, converting remaining oxygenates into hydrocarbons [22]. This sequential process is far more effective than either catalyst acting alone.

In stark contrast, combinations involving the highly acidic zeolite (e.g., Zeo–NiNb) were significantly less effective, yielding a higher proportion of oxygenated intermediates. This is likely due to excessive secondary cracking and coking. The strong Brønsted acid sites of the zeolite can aggressively crack oxygenates into smaller fragments but may also promote polymerization and coke formation, which deactivates the catalyst and prevents complete deoxygenation [40]. This finding underscores the importance of a balanced catalyst functionality; excessive acidity is detrimental, whereas a combination of basicity and moderate redox/acidity (as in the NiNb-PO system) provides the ideal environment for deep bio-oil upgrading.

Across all experiments, nitrogenated compounds were detected only in residual concentrations (0% to 3.3%). This suggests high catalytic efficiency for the thermal decomposition of nitrogen-containing species (likely from proteins in the biomass), primarily converting them into gaseous products such as NH_3 and N_2, which are removed from the liquid phase. This is a positive outcome, as it reduces the potential for NOx emissions if the bio-oil is used as a fuel

4. Conclusions

Microwave-assisted pyrolysis of macauba epicarp (EPM), combined with acidic, basic, and bifunctional catalysts in an ex situ configuration, proved to be a highly promising thermochemical route for the efficient conversion of tropical lignocellulosic residues into upgraded bio-oils. The acid–base nature and surface structure of the catalysts played a crucial role in determining reaction selectivity and product quality.

Among the catalysts evaluated, the bifunctional NiNb–PO system exhibited the best performance, producing the highest hydrocarbon fraction (61.3%) and the lowest proportion of oxygenated compounds (35.4%). This result confirms a synergistic interaction between the redox sites (NiNb) and the basic/multifunctional sites (PO), which is more effective for deoxygenation than individual catalysts. The study elucidated that different catalyst types promote distinct reaction pathways: basic catalysts (CaO, PO) primarily favored decarboxylation and decarbonylation, whereas Nb_2O_5- and NiO/Nb_2O_5-based

systems facilitated selective hydrogenation and deoxygenation. Conversely, highly acidic zeolite-containing combinations favored the formation of oxygenated intermediates, limiting hydrocarbon yield.

The resulting biochar demonstrated high quality, characterized by high fixed carbon content (up to 42.5%), low oxygen content (O/C = 0.24), and a high heating value (21.55 MJ kg^{-1}). Spectroscopic and morphological analyses confirmed the evolution toward a porous and highly aromatic matrix suitable for both energetic and environmental applications.

Overall, this study demonstrates that the integration of multifunctional catalysts, SiC conductive foams, and microwave heating represents a technically feasible and environmentally sustainable approach for producing hydrocarbon-enriched bio-oils and high-performance biochars. The results contribute to advancing the mechanistic understanding of catalytic pyrolysis of tropical biomasses and reinforce the potential of macauba as a strategic resource for the energy transition and next-generation biofuel development

Declarations

Competing Interests

The authors declare no conflicts of interest

Ethical Approval

This article does not contain any studies with human participants or animals performed by any of the authors.

Funding

This research was funded by CAPES, CNPq, and FAPEMIG.

Author Contribution

All authors contributed to the study conception and design. Conceptualization, R.J.C., CR.D., M.A.S.B.; methodology, R.J.C., C.E.H.; writing—original draft preparation, R.J.C. and M.A.S.B.; writing—review and editing, M.A.S.B. and R.J.C.; supervision, M.A.S.B, C.R.D. All authors have read and agreed to the published version of the manuscript.

Acknowledgments

The authors acknowledge the support of the Instituto Federal do Sudeste de Minas Gerais (IF Sudeste MG), the Universidade Federal de Uberlândia (UFU), and the Brazilian funding agencies CNPq, FAPEMIG, and CAPES. The authors also thank CBMM – Companhia Brasileira de Metalurgia e Mineração for providing the niobium oxide used in this study.

Data Availability

The datasets generated during and/or analysed during the current study are available from the corresponding author on reasonable request.

References

1. Bogner J, Pipatti R, Hashimoto S, Diaz C, Mareckova K, Diaz L, Kjeldsen P, Monni S, Faaij A, Qingxian G, Tianzhu Z, Mohammed AA, Sutamihardja RTM, Gregory R (2008) Mitigation of global greenhouse gas emissions from waste: Conclusions and strategies from the intergovernmental panel on climate change (IPCC) fourth assessment report. Waste Manag Res 26(1):11–32. https://doi.org/10.1177/0734242X07088433
2. Cheng H (2020) Future earth and sustainable developments. Innovation 1(3):100055. https://doi.org/10.1016/j.xinn.2020.100055
3. Yang Z, Kumar A, Huhnke RL, Buser M, Capareda S (2021) Pyrolysis of eastern redcedar: Distribution and characteristics of fast and slow pyrolysis products. Fuel 289:119756. https://doi.org/10.1016/j.Fuel.2020119756
4. Queneau Y, Han B (2022) Biomass: Renewable Carbon resource for chemical and energy industry. Innovation 3(1):100184. https://doi.org/10.1016/j.xinn.2021.100184
5. EPE – Empresa de Pesquisa Energéticas (2024) Matriz energética. Accessed 29 February 2024. https://www.epe.gov.br/pt/abcdenergia/matriz-energetica-e-eletrica
6. Cusenza MA, Longo S, Cellura M, Guarino F, Messineo A, Mistretta M, Volpe M (2021) Environmental assessment of a waste-to-energy practice: The pyrolysis of agro-industrial Biomass residues. Sustain Prod Consum 28:866–876. https://doi.org/10.1016/j.spc.2021.07015
7. Promsampao N, Chollacoop N, Pattiya A (2021) Effect of low-temperature hydrothermal treatment of HZSM-5 extrudates on the production of deeply-deoxygenated bio-oil via ex-situ catalytic fast pyrolysis of Biomass. Fuel 324:124627. https://doi.org/10.1016/j.Fuel.2022124627
8. Navarro RM, Guil-Lopez R, Fierro JLG, Mota N, Jiménez S, Pizarro P, Coronado JM, Serrano DP (2021) Catalytic fast pyrolysis of Biomass over Mg-Al mixed oxides derived from hydrotalcite-like precursors: Influence of Mg/Al ratio. J Anal Appl Pyrol 134:362–370. https://doi.org/10.1016/j.jaap.2018.07001
9. Machado H, Cristino AF, Orišková S, Galhano Dos Santos R (2022) Bio-oil: The next-generation source of chemicals. Reactions 3(1):118–137. https://doi.org/10.3390/reactions3010009

10. Liu R, Sarker M, Rahman MM, Li C, Chai M, Nishu, Cotillon R, Scott NR (2020) Multi-scale complexities of solid acid Catalysts in the catalytic fast pyrolysis of Biomass for bio-oil production – A review. Prog Energy Combust Sci 80:100852. https://doi.org/10.1016/j.pecs.2020.100852
11. Zheng Y, Wang F, Yang X, Huang Y, Liu C, Zheng Z, Gu J (2022) Study on aromatics production via the catalytic pyrolysis vapor upgrading of Biomass using metal-loaded modified H-ZSM-5. J Anal Appl Pyrol 126:105044. https://doi.org/10.1016/j.jaap.2017.07011
12. Ratter J (1997) The brazilian cerrado vegetation and threats to its biodiversity. Ann Bot 80(3):223–230. https://doi.org/10.1006/anbo.1997.0469
13. Teixeira VL, Carneiro ADCO, Evaristo AB, Homem De Faria BDF, Donato DB, De Magalhães MA (2018) Potential of macauba epicarp (Acrocomia aculeata (jacq.) Lodd. Ex martius) for briquettes production. Floresta 48(4):563. https://doi.org/10.5380/rf.v48i4.57397
14. Cavallaro RJ, Duarte CR, Hori CE, Barrozo MA (2024) d. S. Optimization of Hydrocarbon Production in Catalytic Pyrolysis of Macaúba Epicarp and Macaúba and Baru Endocarps. Reactions, 5(4), 823–841. https://doi.org/10.3390/reactions5040043
15. Li J, Dai J, Liu G, Zhang H, Gao Z, Fu J, He Y, Huang Y (2016) Biochar from microwave pyrolysis of Biomass: A review. Biomass Bioenergy 94:228–244. https://doi.org/10.1016/j.biombioe.2016.09010
16. Evaristo AB, Grossi JAS, Carneiro ACO, Pimentel LD, Motoike SY, Kuki KN (2016) Actual and putative potentials of macauba palm as feedstock for solid biofuel production from residues. Biomass Bioenergy 85:18–24. https://doi.org/10.1016/j.biombioe.2015.11024
17. Calvani CC, Goncalves A-MB, Silva MJ, Oliveira SL, Marangoni BS, Reis DD, Cena C (2020) Portland cement/acrocomia aculeata endocarp bricks: Thermal insulation and mechanical properties. Materials 13(9):2081. https://doi.org/10.3390/ma13092081
18. Rangel MDC, Mayer FM, Carvalho MDS, Saboia G, Andrade AM (2023) Selecting Catalysts for pyrolysis of lignocellulosic Biomass. Biomass 3(1):31–63. https://doi.org/10.3390/biomass3010003
19. Zhang Z, Pang S, Levi T (2021) Influence of HZSM-5 and Pt/Al2O3 Catalysts on product distribution and hydrogen production during intermediate pyrolysis of radiata pine. J Anal Appl Pyrol 155:105048. https://doi.org/10.1016/j.jaap.2021.105048
20. Li H, Wang Y, Zhou N, Dai L, Deng W, Liu C, Cheng Y, Liu Y, Cobb K, Chen P, Ruan R (2021) Applications of calcium oxide–based Catalysts in Biomass pyrolysis/gasification – A review. J Clean Prod 291:125826. https://doi.org/10.1016/j.jclepro.2021.125826
21. Kulkarni MB, Ghanegaonkar PM (2023) Hydrogen production and Carbon material preparation by catalytic methane decomposition: A comprehensive review. Energy Convers Manag 276:116525. https://doi.org/10.1016/j.enconman.2022.116525
22. Rossi RAS, Dai L, Barrozo MAS, Vieira LGM, Hori CE, Cobb K, Chen P, Ruan R (2023) Bio-Fuel production from catalytic microwave-assisted pyrolysis of the microalgae Schizochytrium limacinum in a tandem catalytic bed. Chem Eng J 478:147223. https://doi.org/10.1016/j.cej.2023.147223

23. Pimenta F, Filho E, Diniz Â, Barrozo MAS (2023) Catalytic microwave-assisted pyrolysis of the main residue of the brewing industry. Catalysts 13(8):1170. https://doi.org/10.3390/catal13081170
24. Lu Q, Zhang Z-F, Dong C-Q, Zhu X-F (2010) Catalytic upgrading of Biomass fast pyrolysis vapors with nano metal oxides: An analytical py-gc/ms study. Energies 3(11):1805–1820. https://doi.org/10.3390/en3111805
25. Nhuchhen DR (2016) Prediction of Carbon, hydrogen, and oxygen compositions of raw and torrefied Biomass using proximate analysis. Fuel 180:348–356. https://doi.org/10.1016/j.Fuel.2016.04058
26. Dourado LRB, Passos JJ, Barbosa JDVB, Araújo TKL, Diniz KM, Neto PQ (2017) Buriti (Mauritia flexuosa L. f.) and macauba (Acrocomia aculeata (Jacq.) Lodd. ex Mart.) oils: Nutritional composition and antioxidant capacity. Cienc Rural 47(8):e20160932. https://doi.org/10.1590/0103-8478cr20160932
27. Raveendran K, Ganesh A, Khilar KC (1996) Pyrolysis characteristics of Biomass and Biomass components. Fuel 75(8):987–998. https://doi.org/10.1016/0016-2361(96)00030-0
28. Aboulkas A, Hammani H, El Achaby M, Bilal E, Barakat A, El Harfi K (2017) Valorization of algal waste via pyrolysis in a fixed-bed reactor: Production and characterization of bio-oil and bio-char. Bioresour Technol 243:400–408. https://doi.org/10.1016/j.biortech.2017.06098
29. Santos KG, Lira TS, Murata VV, Gianesella M, Barrozo MAS (2010) Pyrolysis of sugarcane bagasse: A consecutive Reactions kinetic model from tga experiments. Mater Sci Forum 660–661:593–598. https://doi.org/10.4028/www.scientific.net/MSF.660-661593
30. Chen X, Chen Y, Yang H, Chen W, Wang X, Chen H (2017) Fast pyrolysis of cotton stalk Biomass using calcium oxide. Bioresour Technol 233:15–20. https://doi.org/10.1016/j.biortech.2017.02070
31. Rade LL, Lemos COT, Barrozo MAS, Ribas RM, Monteiro RS, Hori CE (2019) Optimization of esterification reaction over niobium phosphate in a packed bed tubular reactor. Renew Energy 131:348–355. https://doi.org/10.1016/j.renene.2018.07041
32. Xu J, Zhu P, El Azab IH, Bin Xu B, Guo Z, Elnaggar AY, Mersal GAM, Liu X, Zhi Y, Lin Z, Algadi H, Shan S (2022) An efficient bifunctional Ni-Nb2O5 nanocatalysts for the hydrodeoxygenation of anisole. Chin J Chem Eng 49:187–197. https://doi.org/10.1016/j.cjche.2022.07009
33. Skrodczky K, Antunes MM, Han X, Santangelo S, Scholz G, Valente AA, Pinna N, Russo PA (2019) Niobium pentoxide nanomaterials with distorted structures as efficient acid Catalysts. Commun Chem 2(1):129. https://doi.org/10.1038/s42004-019-0231-3
34. Bridgwater AV (2012) Review of fast pyrolysis of Biomass and product upgrading. Biomass Bioenergy 38:68–94. https://doi.org/10.1016/j.biombioe.2011.01048
35. Sierra-Jimenez V, Mathews JP, Yoo P, Budai A, Chejne F, Dufour A, Garcia-Perez M (2024) Biochar data into structure: A methodology for generating large-scale atomistic representations. Carbon 228:119391. https://doi.org/10.1016/j.Carbon.2024119391
36. Deng L, Ye J, Jin X, Che D (2018) Transformation and release of potassium during fixed-bed pyrolysis of Biomass. J Energy Inst 91(4):630–637. https://doi.org/10.1016/j.joei.2017.02009

37. Trazzi PA, Higa AR, Dieckow J, Mangrich AS, Higa RCV (2018) Biocarvão: Realidade e potencial de uso no meio florestal. Cienc Florest 28(2):875–887. https://doi.org/10.5902/1980509832128
38. Zhang Q, Chang J, Wang T, Xu Y (2007) Review of Biomass pyrolysis oil properties and upgrading research. Energy Convers Manag 48(1):87–92. https://doi.org/10.1016/j.enconman.2006.05010
39. Santos GES, Duarte CR, Hori CE, Barrozo MAS (2024) Catalytic pyrolysis of brewer's spent grain in spouted bed reactor using calcium oxide for upgrading oil. J Energy Inst 114:101586. https://doi.org/10.1016/j.joei.2024.101586
40. Andrade LA, Batista FRX, Lira TS, Barrozo MAS, Vieira LGM (2018) Characterization and product formation during the catalytic and non-catalytic pyrolysis of the green microalgae Chlamydomonas reinhardtii. Renew Energy 119:731–740. https://doi.org/10.1016/j.renene.2017.12056

Figures

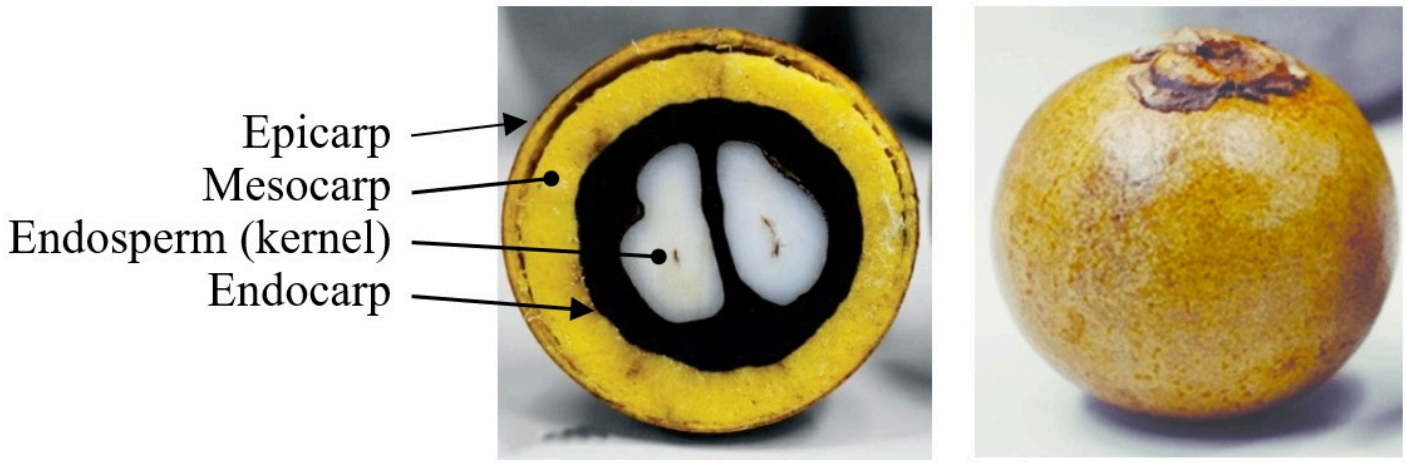

Figure 1

Macaúba fruit – parts of the fruit and whole fruit.

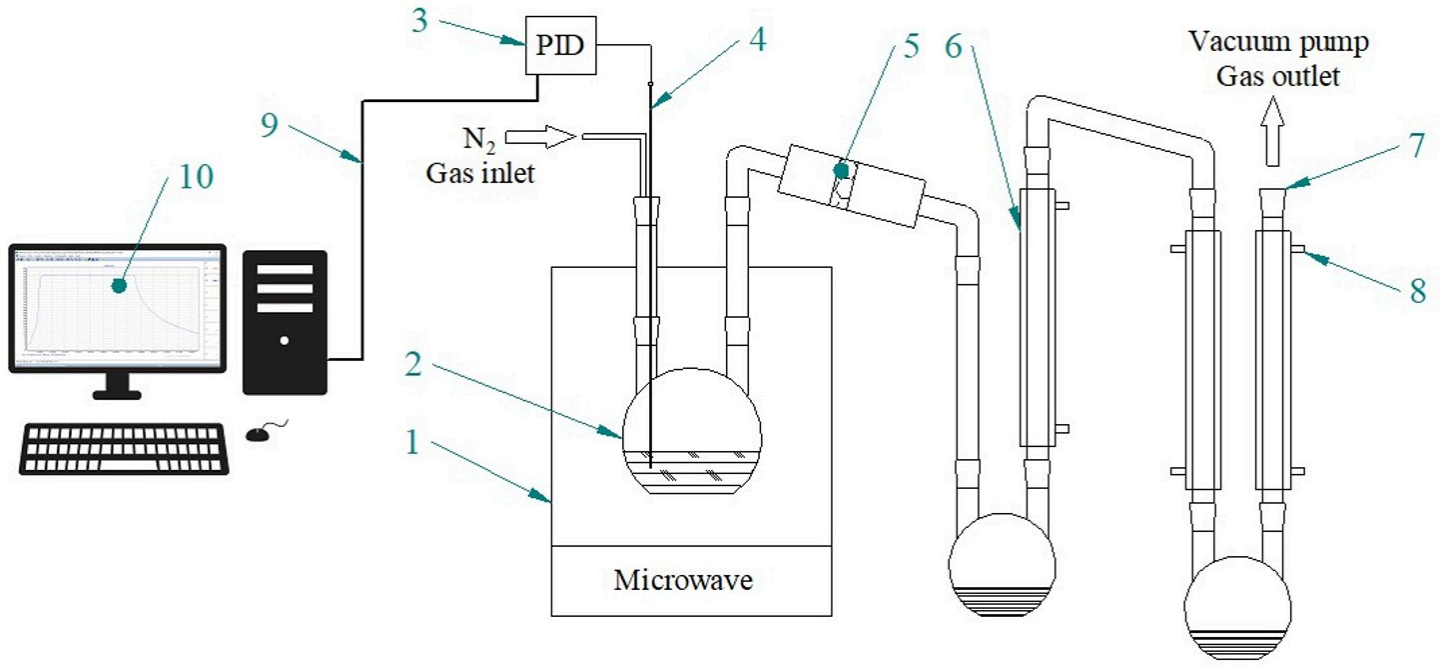

Figure 2

Schematic of the microwave-assisted pyrolysis system.

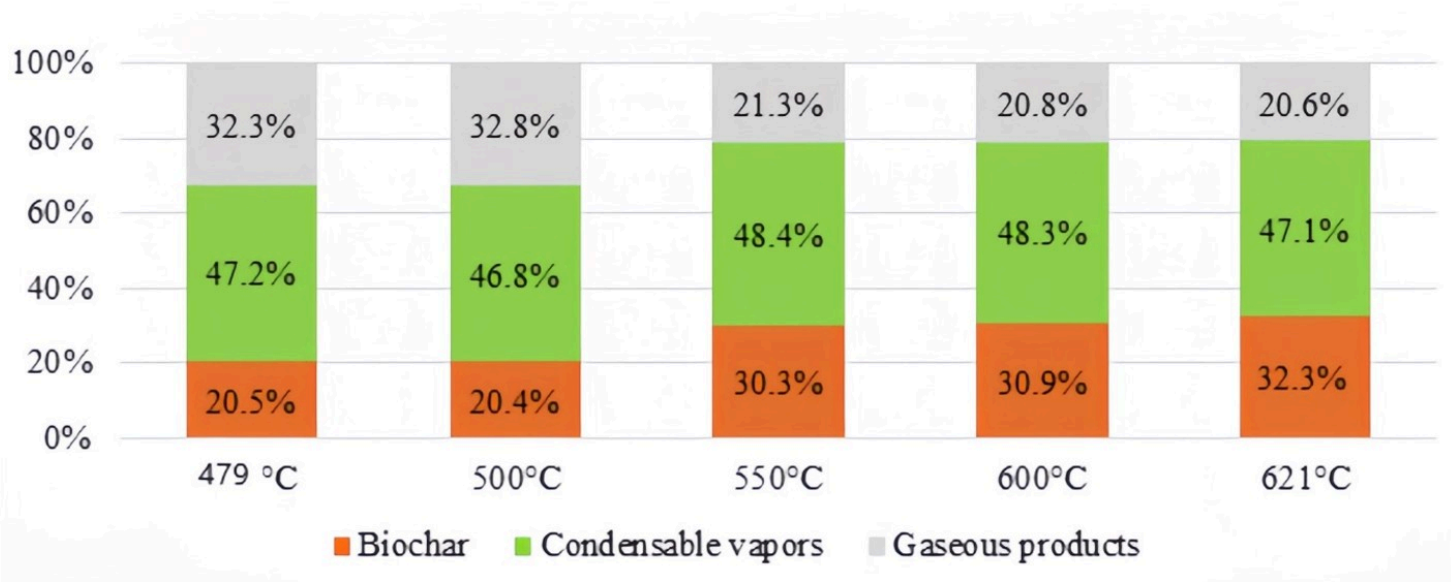

Figure 3

Effect of temperature on product distribution in microwave-assisted non-catalytic pyrolysis of EPM.

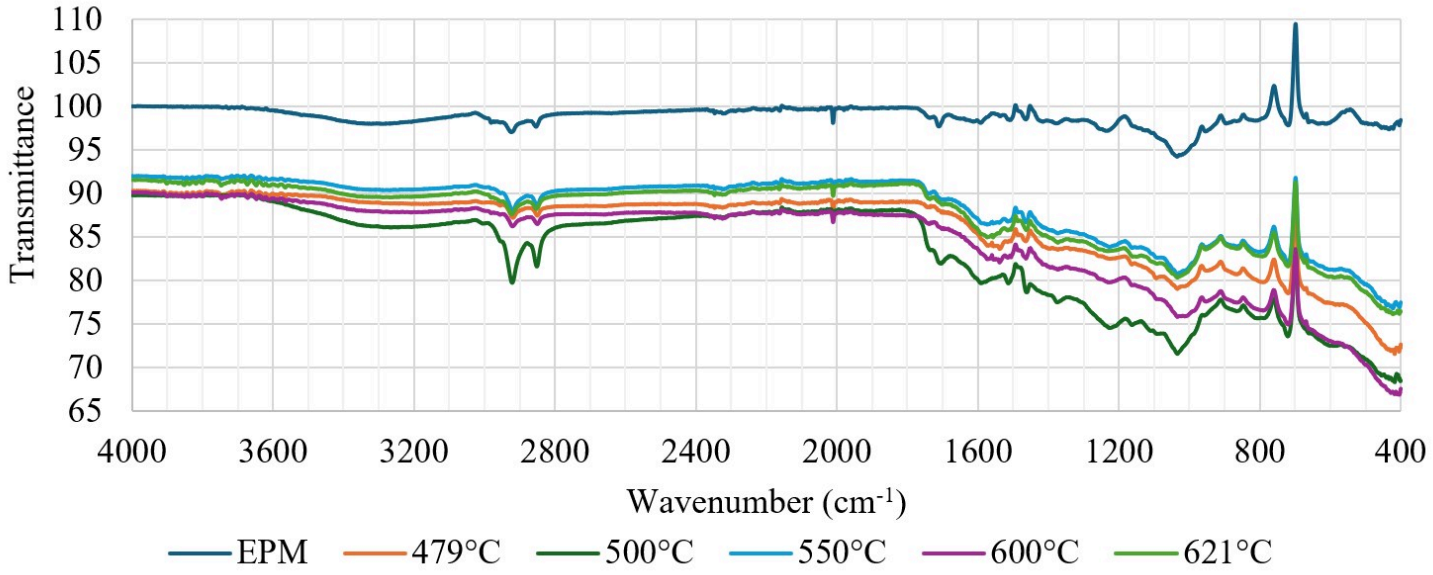

Figure 4

FTIR spectra of EPM biomass and biochars obtained from non-catalytic pyrolysis at different temperatures.

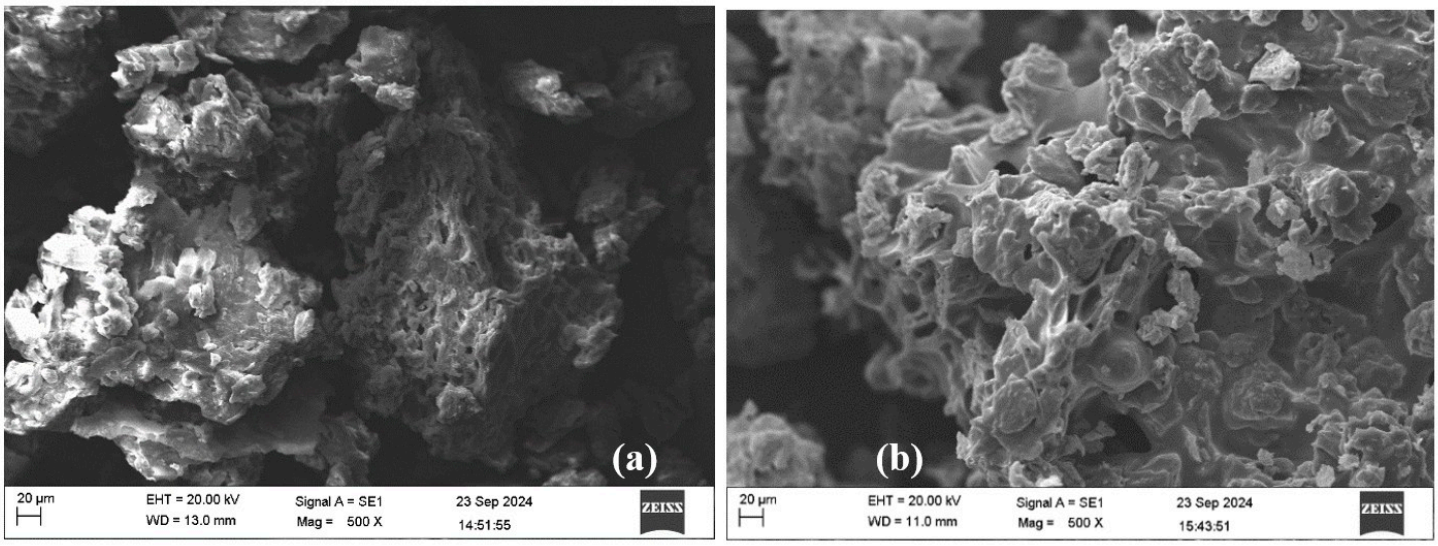

Figure 5

SEM micrographs of (a) raw EPM and (b) biochar at 550°C (magnified 500×).

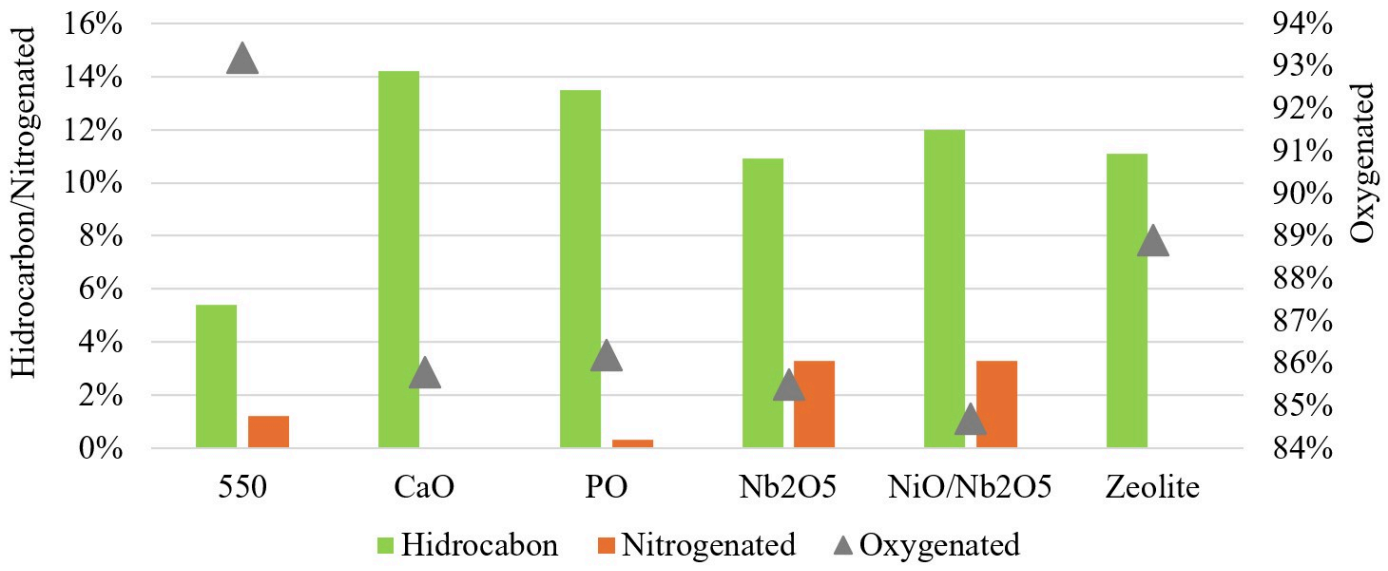

Figure 6

Figure 5. Effect of single catalyst bed on the formation of hydrocarbons, nitrogenated, and oxygenated compounds.

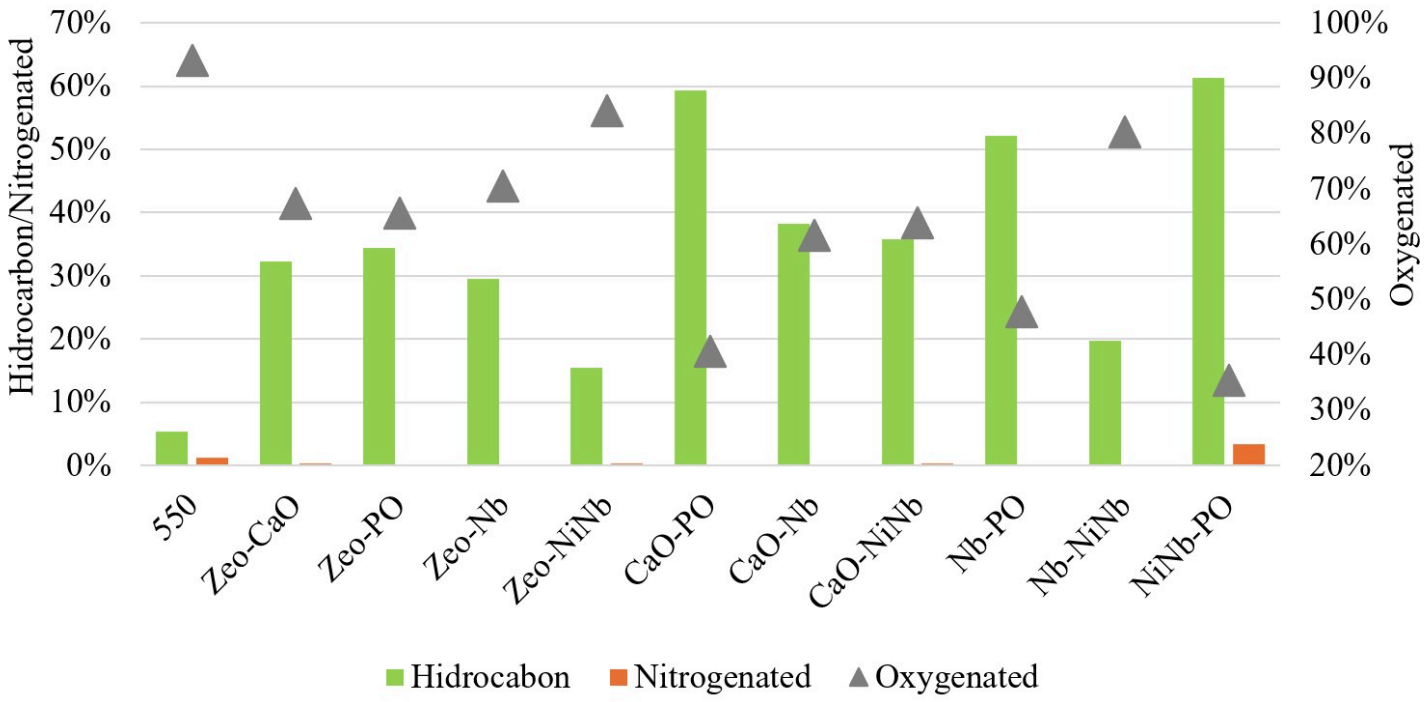

Figure 7

Figure 6. Effect of dual catalyst beds on the formation of hydrocarbons, nitrogenated, and oxygenated compounds.